

ELECTRICAL PROPERTIES OF $\text{Li}_{1.3}\text{M}_{1.4}\text{Ti}_{0.3}\text{Al}_{0.3}(\text{PO}_4)_3$ ($\text{M} = \text{Ge}, \text{Zr}$) SUPERIONIC CERAMICS*

E. Kazakevičius^a, A. Určinskas^a, B. Bagdonas^a, A. Kežionis^a, A.F. Orliukas^a,
A. Dindune^b, Z. Kanepe^b, and J. Ronis^b

^a Faculty of Physics, Vilnius University, Saulėtekio 9, LT-10222 Vilnius, Lithuania

E-mail: edvardas.kazakevicius@ff.vu.lt

^b Institute of Inorganic Chemistry, Riga Technical University, Miera 34, LV-2169 Salaspils, Latvia

Received 25 July 2005

Preparation and electrical characterization of compounds $\text{Li}_{1.3}\text{Ge}_{1.4}\text{Ti}_{0.3}\text{Al}_{0.3}(\text{PO}_4)_3$ and $\text{Li}_{1.3}\text{Zr}_{1.4}\text{Ti}_{0.3}\text{Al}_{0.3}(\text{PO}_4)_3$, are described. The solid solutions are obtained with $\text{M}^{4+} \rightarrow \text{Ti}^{4+}$ and $\text{M}^{4+} \rightarrow \text{Al}^{3+}$ substitutions in $\text{LiM}_2(\text{PO}_4)_3$ (where $\text{M} = \text{Ge}, \text{Zr}$). The powders have been fabricated by a solid state reaction and their structural characteristics have been studied by X-rays. Ceramic samples have been sintered by varying the sintering duration from 1 to 3 hours. Samples were studied by complex impedance spectroscopy in the frequency range 1 MHz–1.2 GHz and temperature range 300–600 K. Two regions of relaxation dispersion were found. The dispersions were related to the fast Li^+ ion transport in the grains and grain boundaries. Variation of the sintering duration has no considerable effect on electrical properties of the ceramics.

Keywords: solid electrolyte ceramics, ionic conductivity, synthesis, transport properties

PACS: 61.10.Nz, 66.30.Hs, 81.05.Je, 82.45.Yz

1. Introduction

Na^+ ion conductive compounds with NASICON-type framework were discovered and synthesized primarily for energy storage applications [1]. Also, they were proposed for sensor devices because of interesting selectivity properties [2]. Subsequent investigations of lithium ion conductors were made using systems $\text{LiM}_2(\text{PO}_4)_3$ ($\text{M} = \text{Zr}, \text{Ti}, \text{Hf}, \text{Ge}$) [3–6]. The interest was focused mainly on systems $\text{Li}_{1+x}\text{M}_x\text{Ti}_{2-x}(\text{PO}_4)_3$ ($\text{M} = \text{Sc}, \text{Al}, \text{Fe}, \text{Y}$) [5, 7, 8], $\text{Li}_{1+x}\text{M}_x\text{Ge}_{2-x}(\text{PO}_4)_3$ ($\text{M} = \text{Al}, \text{Cr}, \text{Ga}, \text{Fe}, \text{Sc}$) [6, 9, 10], and $\text{Li}_{1+x}\text{M}_x\text{Zr}_{2-x}(\text{PO}_4)_3$ ($\text{M} = \text{Sc}, \text{Ti}, \text{Hf}, \text{Ta}, \text{Nb}$) [3, 5, 11–13], where ionic conductivities were found to be several orders of magnitude higher than in host compounds. Some of these materials were also incorporated in sensor devices [9, 14] and the advantage of Li^+ electrolytes against Na^+ ones for usage in biomedical applications was revealed [15]. The compounds with both Ge^{4+} and Ti^{4+} , or Zr^{4+} and Ti^{4+} cations included in composition of the phosphates were also investigated [5, 11, 16–18]. Despite of an unalterable concentration of mobile ions, the conductivity

of $\text{LiGe}_{2-x}\text{Ti}_x(\text{PO}_4)_3$ and $\text{LiZr}_{2-x}\text{Ti}_x(\text{PO}_4)_3$ increases by several orders of magnitude with x rising from 0 to 2 [5, 16]. The phase transitions which were observed in $\text{LiZr}_2(\text{PO}_4)_3$ at about room and 560 K temperatures [18–20] shifted to lower temperature regions or even were not observed in the case of $\text{LiZr}_{2-x}\text{Ti}_x(\text{PO}_4)_3$ system [5, 11, 18]. The NASICON crystallographic structure was first identified by Hagman and Kierkegaard [21]. The usual structure is rhombohedral, space group $R\bar{3}c$, but in some particular cases the compounds also show a low temperature phase of monoclinic symmetry [1, 19, 22]. The framework is built up of $\text{M}_2(\text{PO}_4)_3$ units in which two MO_6 octahedra and three PO_4 tetrahedra share oxygen atoms. They form conducting channels and two types of interstitial spaces where conductor cations are distributed. In the rhombohedral lithium phases, such as $\text{LiGe}_2(\text{PO}_4)_3$, $\text{LiTi}_2(\text{PO}_4)_3$, and $\text{LiZr}_2(\text{PO}_4)_3$, the preferential occupancy of one type of sites by lithium has been pointed out by neutron diffraction experiments [23, 24]. The conductor cations move from one site to another through the channels the size of which depends on a nature of skeleton ions and on the carrier concentration in both types of sites. Consequently, the structural and electrical properties of NASICON-type compounds vary with the compo-

* The report presented at the 36th Lithuanian National Physics Conference, 16–18 June 2005, Vilnius, Lithuania.

sition of the framework. For example, in the compounds of general formula $\text{LiM}_{2-x}\text{A}_x(\text{PO}_4)_3$ the cell parameters a and c depend on the M and A cation sizes [16]. The smallest unit cell has been obtained in $\text{LiGe}_2(\text{PO}_4)_3$. Incorporation of a trivalent cation into $\text{LiGe}_{2-x}\text{Ti}_x(\text{PO}_4)_3$ and $\text{LiZr}_{2-x}\text{Ti}_x(\text{PO}_4)_3$ frameworks seems to be a good choice for a study.

We report the investigation of structure and electrical properties of $\text{Li}_{1.3}\text{Ge}_{1.4}\text{Ti}_{0.3}\text{Al}_{0.3}(\text{PO}_4)_3$ and $\text{Li}_{1.3}\text{Zr}_{1.4}\text{Ti}_{0.3}\text{Al}_{0.3}(\text{PO}_4)_3$ compounds (indicated in text as Ge-comp and Zr-comp, respectively). The materials were fabricated by a solid state reaction (SSR). The structures were examined by X-ray diffraction and several ceramic samples were sintered for investigation of electrical properties by impedance spectroscopy. The present work continues our study of Li^+ and Na^+ superionic ceramics [25–30].

2. Experimental

Published results concerning the mentioned materials usually have been related to these prepared by a SSR [6, 7, 16]. The authors of Refs. [9, 14] have developed a sol-gel method for preparation of $\text{Li}_{1+x}\text{M}_x\text{Ti}_{2-x}(\text{PO}_4)_3$ (with x from 0 to 0.7). The conductivity of ceramics sintered in this way was about one order of magnitude lower than that prepared by SSR. The authors of [9] have supposed that this difference could be due to the presence of LiTiOPO_4 phase at grain boundaries. The advantage of sol-gel is that the determined composition generally better agrees with stoichiometric formula as compared to SSR ceramics [9]. $\text{LiZr}_2(\text{PO}_4)_3$ based compounds were also synthesized by sol-gel [12, 20]. In the present work the SSR was used for the synthesis of Ge-comp and Zr-comp. The powders were prepared from stoichiometric mixtures of Al_2O_3 (purity 99.999%), Li_2CO_3 (99.999%), TiO_2 , GeO_2 (or ZrO_2), and $\text{NH}_4\text{H}_2\text{PO}_4$ (extra pure). The synthesis of the compounds followed this sequence: calcination at $T = 450^\circ\text{C}$ for 20 h; milling with ethanol in a ball mill for 12 h; then the calcination at 1000 – 1020°C for 8 h jointly and grinding in agate mortar was repeated 3 times in turn. Finally, the powders were calcinated for 3 h at 1100°C for the Ge-comp and for 1 h at 1220°C for the Zr-comp. The structure parameters were obtained using X-ray diffraction (Cu K_α radiation at room temperature in air) from the powder. A suitable amount of polypropyleneglycol solution was added to the powders as a binder, and the mixtures were uniaxially pressed into pellets at 300 MPa. The shrinkage

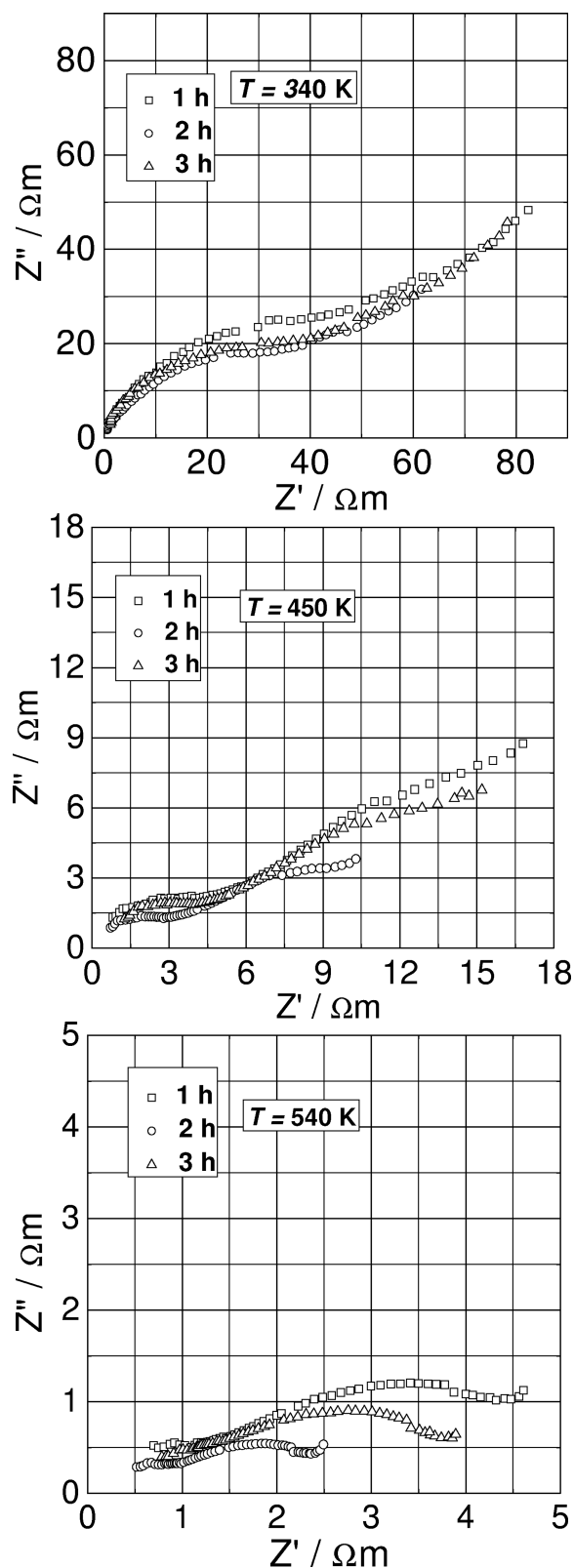


Fig. 1. Complex impedance plots at different temperatures T of Ge-comp ceramics produced with various sintering durations.

was monitored as a function of temperature to allow the optimization of sintering conditions. Three

Table 1. Hexagonal unit cell parameters, volume, and density. Ionic radii of the skeleton cations are also included [31].

Compound	Cell parameters, Å		Cell volume V , Å ³	Density, g/cm ³	Ionic radii, Å
	a	c			
LiGe ₂ (PO ₄) ₃	8.25	20.46	1205.99	3.61	Ge ⁴⁺ : 0.53
LiTi ₂ (PO ₄) ₃	8.5129(8)	20.878(4)	1310.3	2.948	Ti ⁴⁺ : 0.605
LiZr ₂ (PO ₄) ₃	8.8077	22.715	1526.05	3.10	Zr ⁴⁺ : 0.8
Li _{1.3} Ge _{1.4} Ti _{0.3} Al _{0.3} (PO ₄) ₃	8.31(3)	20.496(12)	1225.85	3.397	Al ³⁺ : 0.535
Li _{1.3} Zr _{1.4} Ti _{0.3} Al _{0.3} (PO ₄) ₃	8.803(3)	21.882(4)	1468.47	3.013	Al ³⁺ : 0.535

pressed powder pellets of each compound were heated at 400 °C for 1 h to eliminate adsorbed water and to avoid ceramic cracks. Ceramics were sintered in air at 1100 °C for Ge-comp and at 1290 °C for Zr-comp, each for several sintering durations ($t_s = 1, 2$, and 3 h). The measurements of complex impedance ($\tilde{Z} = Z' - iZ''$) and complex electric conductivity ($\tilde{\sigma} = \sigma' - i\sigma''$) were done by means of coaxial impedance spectrometer set-up in the frequency range $1 \cdot 10^6$ Hz – $1.2 \cdot 10^9$ Hz. The ceramic samples were 2 mm in diameter and 1.5 mm thick. The samples were covered with Pt electrodes [26].

3. Results and discussion

The results of X-ray diffraction study have shown that the typical X-ray peaks of the reagents were not detected, nonetheless a small amount of intermediate SSR compound AlPO₄ was found in Ge-comp and, respectively, ZrP₂O₉ in Zr-comp. The symmetry is rhombohedral with a space group $R\bar{3}c$ and six formula units in the unit cell. The cell parameters (hexagonal unit) of compounds together with those of LiGe₂(PO₄)₃, LiZr₂(PO₄)₃, and LiTi₂(PO₄)₃ are presented in Table 1.

The X-ray diffraction study shows clearly that the evolutions of cell parameters and volume can be interpreted as a qualitative function of the ionic radius of the cation in octahedral sites. The Ge → Ti, Al substitutions lead to an increase of these parameters, what is consistent with the results in Refs. [5–7]. The Zr → Ti, Al substitutions lead to a decrease of values of these parameters, and this is consistent with results obtained in Refs. [5, 10]. Several phenomena may play a determining role in the influence of the cationic substitution on the structure and ionic conductivity of NASICON-type materials [1, 5, 32]. The observed increase could be attributed to the occupancy of the conduction sites, when Al³⁺ and subsequently Li⁺ doping takes place. The additional Li⁺ ions are localized in one type of sites, while another type is occupied minimally; consequently, this

leads to a maximal repulsion along the c axis as it is in Na⁺-NASICON [1].

The quality of ceramic samples (porosity and grain boundary phase) plays a major role in the conductive properties [6, 7, 9, 16], and our samples of different sintering duration contained a satisfying fraction of the theoretical density (see Table 1): 86% for $t_s = 1$ h, 79% for $t_s = 2$ h, 72% for $t_s = 3$ h for the Ge-comp. The observed decrease of the relative density can be associated with a leakage of glass phase during the sintering of ceramics. The continuous sintering produces the larger amount of leakage products which are found in the furnace on the substrate for pellets. The glass phase in grain boundaries seems to diminish, leaving room for crystallite growth or cavity formation that could be responsible for the decrease of density, i. e. the increase of porosity. In the case of Zr-comp, the relative density has not changed during 3 hours of sintering and stayed at value of 80%. Probably a longer duration of sintering is necessary to observe some effects.

Two dispersive regions were observed in impedance spectra of ceramics. They both shift towards a high-frequency range when the temperature is increased. We relate these dispersions with two thermally activated relaxation processes, the ion transport in grains and the ion transport in grain boundaries. We managed to suit some of the impedance plots (Fig. 1) to equivalent circuit elements using nonlinear least squares fits [33]. The equivalent circuits consisted of two parallel combinations of resistance, capacitance, and constant phase element in series. The admittance of constant phase element is given by the formula $Y_{CPE} = Y(j\omega)^n$ [33]. The mentioned sub-circuits describe the bulk or grain boundary properties of the samples. The value of above capacitance, which in parallel with resistance roughly reproduces the observed dispersion, has been advocated in Ref. [33] as a key to identification of the physical origin of the process. Approximate values of capacitances were calculated from the frequencies of maxima of $Z''(f)$ spectra (Fig. 2) or, alternatively, the complex modulus plots were helpful in characterization of

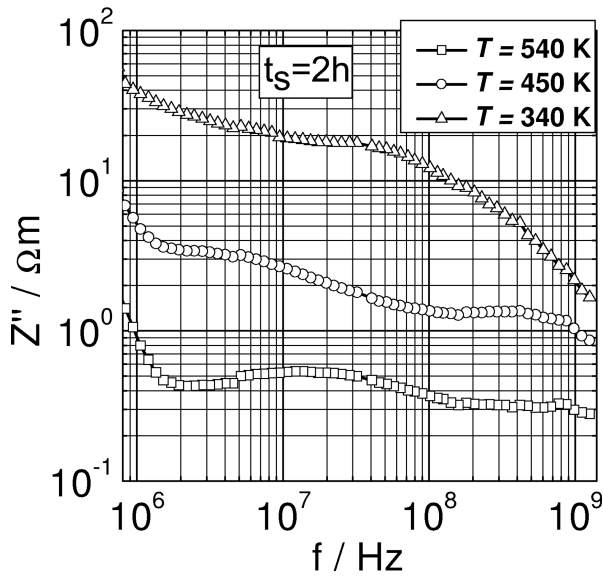


Fig. 2. Imaginary impedance ($-Z''$) versus frequency for Ge-comp ceramic with sintering duration 2 h.

dispersion caused by grain boundaries [34]. In the case of Ge-comp the approximate values of capacitances associated with high/low frequency arcs in the impedance plots (Fig. 1) of the sample show that the high frequency arc is associated with the grain response, while the low frequency arc is associated with the grain boundaries. In the case of Zr-comp the dispersive regions were overlapped and hard to separate. The total (σ_t), grain (σ_g), and grain boundary (σ_{gb}) dc conductivities were calculated from corresponding impedance values determined from the impedance plots (Fig. 1). In the case of Zr-comp, it was possible to determine only the values of σ_t . The Arrhenius plots for total and bulk conductivities are shown in Fig. 3. The values of conductivities σ_t , σ_g at different temperatures and their activation energies E_t , E_g are given in Table 2.

Due to the limits of frequency range used, it was not possible to determine total and grain conductivities of Ge-comp for the same temperature ranges, however, from Fig. 3 it is seen that the overall conductivity is generally lower than the one due to grains. This proves that the total conductivity is mostly dominated by the grain boundary contribution as reported by authors of [7, 9].

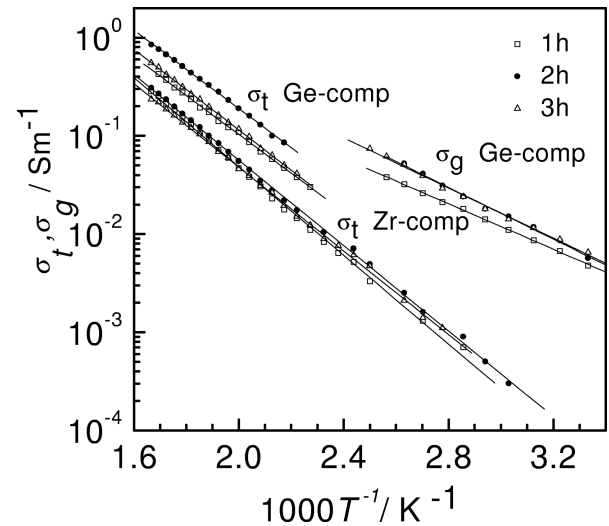


Fig. 3. Arrhenius plots of the total and grain conductivities for Ge-comp and Zr-comp.

This blocking effect in grain boundaries could be correlated with the porosity of the samples [7], but in our case it has been shown that a higher duration of sintering results in a lower relative density of ceramics, and we can see no correlation of density with conductivities and activation energies. The total conductivity of 2 h sintered ceramics is slightly higher than that of other samples, but in general the sintering duration has no effect on electrical properties. Comparison of Ge-comp with other NASICON-type materials shows that the conductivities are similar to those of $\text{Li}_{1.5}\text{Ge}_{1.5}\text{Al}_{0.5}(\text{PO}_4)_3$ [6], which has been reported to have the highest conductivity in $\text{Li}_{1+x}\text{Ge}_{2-x}\text{Al}_x(\text{PO}_4)_3$ system. The total conductivity of the investigated compound is an order of magnitude lower than that of $\text{Li}_{1.3}\text{Ti}_{1.7}\text{Al}_{0.3}(\text{PO}_4)_3$, and this proves that Ti-based network is better calibrated for Li^+ motion than Ge-based one. This is because $\text{LiGe}_2(\text{PO}_4)_3$ crystalline cell is too small to permit an optimal Li^+ motion [9]. As reported in [5], the total conductivity of $\text{LiZr}_{2-x}\text{Ti}_x(\text{PO}_4)_3$ system at 573 K increases from $2.1 \cdot 10^{-3}$ S/m to $5 \cdot 10^{-1}$ S/m when x rises from 0 to 2. The total conductivity of Zr-comp ceramics is about $1.9 \cdot 10^{-1}$ S/m, so the substitution $\text{Zr}^{4+} \rightarrow \text{Al}^{3+}$ leads to increase of total conduc-

Table 2. Total and grain conductivities at different temperatures and their activation energies for ceramics of various sintering durations.

t_s , h	$\text{Li}_{1.3}\text{Ge}_{1.4}\text{Ti}_{0.3}\text{Al}_{0.3}(\text{PO}_4)_3$						$\text{Li}_{1.3}\text{Zr}_{1.4}\text{Ti}_{0.3}\text{Al}_{0.3}(\text{PO}_4)_3$		
	σ_t (500 K), S/m	σ_t (600 K), S/m	E_t , eV	σ_g (300 K), S/m	σ_g (380 K), S/m	E_g , eV	σ_t (500 K), S/m	σ_t (600 K), S/m	E_t , eV
1	$1.1 \cdot 10^{-1}$	$4.8 \cdot 10^{-1}$	0.39	$4.8 \cdot 10^{-3}$	$3.2 \cdot 10^{-2}$	0.23	$4.66 \cdot 10^{-2}$	$2.8 \cdot 10^{-1}$	0.45
2	$1.9 \cdot 10^{-1}$	$8.5 \cdot 10^{-1}$	0.40	$5.7 \cdot 10^{-3}$	$5.2 \cdot 10^{-2}$	0.26	$5.53 \cdot 10^{-2}$	$3.1 \cdot 10^{-1}$	0.44
3	$1.2 \cdot 10^{-1}$	$5.5 \cdot 10^{-1}$	0.40	$6.5 \cdot 10^{-3}$	$5.1 \cdot 10^{-2}$	0.25	$4.59 \cdot 10^{-2}$	$2.4 \cdot 10^{-1}$	0.43

tivity, mostly due to increased content of Li^+ . The fundamental interest would be to expand the present investigations to systems like $\text{Li}_{1+x}\text{Ge}_{2-x-y}\text{Ti}_y\text{Al}_x(\text{PO}_4)_3$ and $\text{Li}_{1+x}\text{Zr}_{2-x-y}\text{Ti}_y\text{Al}_x(\text{PO}_4)_3$ with properly varying x and y in a wide range. A small amount of dopant Ti^{4+} used in our case has no noticeable effect on the conductivity. The positive point of the study of Ge-comp is that a more confined unit cell is appropriate for selective behaviour in ion selective electrodes, although it is less conductive than Ti-based [9] one.

The relaxation frequencies (f_g) that determine the relaxation dispersion process in grains of Ge-comp were obtained from the maxima of the $Z''(f)$ spectra at different temperatures (Fig. 2). The increase of f_g was fitted to the expression $f_g = f_0 \exp(E_f/(kT))$, where f_0 is an attempt frequency and E_f is the activation energy of the process. We have deduced from the impedance spectra that this frequency is very close to the hopping rate of ions [35]. Also, the values of E_f were found to be similar to those of E_g (Table 2). This fact confirms that the temperature dependence of σ_g is caused only by the mobility of the fast Li^+ ions, while the number of charge carriers remains constant with the variation of sample temperature.

4. Conclusions

The new materials, $\text{Li}_{1.3}\text{Ge}_{1.4}\text{Ti}_{0.3}\text{Al}_{0.3}(\text{PO}_4)_3$ and $\text{Li}_{1.3}\text{Zr}_{1.4}\text{Ti}_{0.3}\text{Al}_{0.3}(\text{PO}_4)_3$, exhibit good electrolytic properties. Therefore, the main interest is to expand the investigations to systems $\text{Li}_{1+x}\text{Ge}_{2-x-y}\text{Ti}_y\text{Al}_x(\text{PO}_4)_3$ where small amount of dopant Ti^{4+} has no noticeable effect on conductivity. Two regions of the obtained impedance dispersion of the ceramics have been found and associated with fast lithium ion transport in the grains and grain boundaries. The evolution of unit cell parameters and volume can be interpreted as a qualitative function of the ionic radius of the cation in octahedral sites. The charge transport in the investigated compounds may be described mainly by the temperature dependent ion mobility. The sintering duration of ceramics has been found to have no effect on the electrolytic properties.

References

- [1] J.B. Goodenough and H.P.Y. Hong, *Mater. Res. Bull.* **11**, 203–220 (1976).
- [2] P. Fabry, J.P. Gros, and M. Kleitz, *Solid state ionics for ISFETs*, in: *Symposium of Electrochemical Sensors* (Rome, 12–14 June, 1984).
- [3] B.E. Taylor, A.D. English, and T. Berzins, *Mater. Res. Bull.* **12**, 171–181 (1977).
- [4] S.-C. Li and Z.-Z. Lin, *Solid State Ionics* **9/10**, 835–837 (1983).
- [5] M.A. Subramanian and R. Subramanian, *Solid State Ionics* **18/19**, 562–569 (1986).
- [6] S.-C. Li, J.-Y. Cai, and Z.-X. Lin, *Solid State Ionics* **28/30**, 1265–1270 (1988).
- [7] H. Aono, E. Sugimoto, Y. Sadaoka, N. Imanaka, and G. Adachi, *J. Electrochem. Soc.* **137**, 1023–1027 (1990).
- [8] Y. Saito, K. Ado, H. Kageyama, and O. Nakamura, *J. Mater. Sci. Lett.* **11**, 888–890 (1992).
- [9] M. Cretin and P. Fabry, *J. Eur. Ceram. Soc.* **19**, 2931–2940 (1999).
- [10] H. Aono, E. Sugimoto, Y. Sadaoka, N. Imanaka, and G. Adachi, *J. Electrochem. Soc.* **140**, 1827–1833 (1993).
- [11] J. Kuwano, N. Sato, M. Kato, and K. Takano, *Solid State Ionics* **70/71**, 332–336 (1994).
- [12] M. Barj, H. Perthuis, and Ph. Colomban, *Solid State Ionics* **9/10**, 845–850 (1983).
- [13] B.V.R. Chowdari, K. Radhakrishnan, K.A. Thomas, and G.V. Subba Rao, *Mater. Res. Bull.* **24**, 221–229 (1989).
- [14] M. Cretin, P. Fabry, and L. Abello, *J. Eur. Ceram. Soc.* **15**, 1149–1156 (1995).
- [15] M. Cretin and P. Fabry, *Anal. Chim. Acta* **357**, 291–299 (1997).
- [16] J.-M. Winand, A. Rulmond, and P. Tarte, *J. Solid State Chem.* **93**, 341–349 (1991).
- [17] H. Aono, E. Sugimoto, Y. Sadaoka, N. Imanaka, and G. Adachi, *Bull. Chem. Soc. Jpn.* **65**, 2200–2204 (1992).
- [18] M. Casiola, U. Constantino, I.G. Krogh Andersen, and E. Krogh Andersen, *Solid State Ionics* **37**, 281–287 (1990).
- [19] F. Sudreau, D. Petit, and J.P. Boilot, *J. Solid State Chem.* **83**, 78–90 (1989).
- [20] D. Petit, Ph. Colomban, G. Collin, and J.P. Boilot, *Mater. Res. Bull.* **21**, 365–371 (1986).
- [21] L.O. Hagman and P. Kierkegaard, *Acta Chem. Scand.* **22**, 1822–1832 (1968).
- [22] S. Hamdoune, M. Gondran, and D. Tran Qui, *Mat. Res. Bull.* **21**, 237–242 (1986).
- [23] D. Tran Qui, S. Hamdoune, and J.L. Soubeyroux, *J. Solid State Chem.* **72**, 309–315 (1988).
- [24] M. Catti and S. Stramare, *Solid State Ionics* **136–137**, 489–494 (2000).
- [25] A. Dindune, A. Kežionis, Z. Kanepe, E. Kazakevičius, R. Sobiestianskas, and A. Orliukas, *Phosphorus Res. Bull.* **10**, 387–392 (1999).
- [26] R. Sobiestianskas, A. Dindune, Z. Kanepe, J. Ronis, A. Kežionis, E. Kazakevičius, and A. Orliukas, *Mater. Sci. Eng. B* **76**, 184–192 (2000).

- [27] W. Bogusz, J.R. Dygas, F. Krok, A. Kezionis, R. Sobiestianskas, E. Kazakevičius, and A. Orliukas, *Phys. Status Solidi A* **183**, 323–330 (2001).
- [28] A. Dindune, E. Kazakevičius, Z. Kanepe, J. Ronis, A. Kežionis, and A. Orliukas, *Phosphorus Res. Bull.* **13**, 107–110 (2002).
- [29] A. Dindune, Z. Kanepe, E. Kazakevičius, A. Kežionis, J. Ronis, and A.F. Orliukas, *J. Solid State Electrochem.* **7**, 113–117 (2003).
- [30] A. Orliukas, A. Dindune, Z. Kanepe, J. Ronis, E. Kazakevičius, and A. Kežionis, *Solid State Ionics* **157**, 177–181 (2003).
- [31] R.D. Shanon, *Acta Crystallogr. A* **32**, 751–767 (1976).
- [32] C. Delmas, J.C. Viala, R. Olazcuaga, G. Le Flem, and P. Hagenmuller, *Mat. Res. Bull.* **16**, 83–90 (1981).
- [33] J.R. Macdonald, *Impedance Spectroscopy* (Wiley, New York, 1987).
- [34] J.G. Fletcher, A.R. West, and J.T.S. Irvine, *J. Electrochem. Soc.* **142**, 2650–2654 (1995).
- [35] D.P. Almond, G.K. Duncan, and A.R. West, *Solid State Ionics* **8**, 159–164 (1983).

ELEKTRINĖS SUPERJONINIŲ KERAMIKŲ $\text{Li}_{1,3}\text{M}_{1,4}\text{Ti}_{0,3}\text{Al}_{0,3}(\text{PO}_4)_3$ ($\text{M} = \text{Zr}, \text{Ge}$) SAVYBĖS

E. Kazakevičius^a, A. Určinskas^a, B. Bagdonas^a, A. Kežionis^a, A.F. Orliukas^a, A. Dindune^b, Z. Kanepe^b, J. Ronis^b

^a Vilniaus universitetas, Vilnius, Lietuva

^b Rygos technikos universiteto Neorganinės chemijos institutas, Salaspilis, Latvija

Santrauka

Joninis junginių $\text{LiZr}_2(\text{PO}_4)_3$ ir $\text{LiGe}_2(\text{PO}_4)_3$ laidumas yra palyginti mažas, tačiau Zr^{4+} ir Ge^{4+} katijonų daliniai keitimai kitais katijonais gali net keliomis eilėmis jį padidinti. Yra paskelbta nemažai darbų, kuriuose buvo tirtos medžiagos, gautos keičiant $\text{Zr}^{4+} \rightarrow \text{Sc}^{3+}$, Ti^{4+} , Hf^{4+} , Ta^{4+} ir $\text{Ge}^{4+} \rightarrow \text{Al}^{3+}$, Cr^{3+} . Pavyzdžiui, $\text{Li}_{1,5}\text{Ge}_{1,5}\text{Al}_{0,5}(\text{PO}_4)_3$ laidumas kambario temperatūroje yra $3,5 \cdot 10^{-3} \text{ S/m}$, nors pradinės medžiagos $\text{LiGe}_2(\text{PO}_4)_3$ laidumas tesiekia $3 \cdot 10^{-5} \text{ S/m}$. Dalinai keičiant Zr^{4+} ar Ge^{4+} tokio pat valentingumo katijonais, laidumas taip pat kinta. Pavyzdžiui, junginių sistemos $\text{LiGe}_{2-x}\text{Ti}_x(\text{PO}_4)_3$ laidumo vertės padidėja keliomis eilė-

mis, x kintant nuo 0 iki 2. Minėti darbai paskatino pagaminti naujus sudėtingus junginius, Zr^{4+} ir Ge^{4+} dalinai keičiant iš karto dviem katijonais, Al^{3+} ir Ti^{4+} . Junginiai $\text{Li}_{1,3}\text{Zr}_{1,4}\text{Ti}_{0,3}\text{Al}_{0,3}(\text{PO}_4)_3$ ir $\text{Li}_{1,3}\text{Ge}_{1,4}\text{Ti}_{0,3}\text{Al}_{0,3}(\text{PO}_4)_3$ buvo sintezuoti kietųjų fazių reakcijoje, o jų kristalinė sandara tirta naudojant Röntgen'o spinduliuotės difrakciją. Buvo pagaminta keletas skirtingą laiko tarpą kepintų keramikinių bandinių ir jų elektrinės savybės ištirtos 1–1250 MHz dažnių elektriniuose laukuose, 300–600 K temperatūros tarpe. Tirtose keramikose stebimi du relaksacijos vyksmai, susiję su jonų pernaša kristalituose ir tarpkristalitinėje terpėje.